Journal of Human Evolution xxx (2013) 1–17

Contents lists available at SciVerse ScienceDirect

Journal of Human Evolution

journal homepage: www.elsevier.com/locate/jhevol

Review

Combined ESR/U-series chronology of Acheulian hominid-bearing layers at Trinchera Galería site, Atapuerca, Spain

Christophe Falguères [a,*], Jean-Jacques Bahain [a], James L. Bischoff [b], Alfredo Pérez-González [c], Ana Isabel Ortega [c], Andreu Ollé [d,e], Anita Quiles [f], Bassam Ghaleb [g], Davinia Moreno [a,d], Jean-Michel Dolo [h], Qingfeng Shao [a], Josep Vallverdú [d,e], Eudald Carbonell [d,e,i], Jose María Bermúdez de Castro [c], Juan Luis Arsuaga [j]

[a] *Département de Préhistoire, Muséum national d'histoire naturelle, UMR7194, 1, rue René Panhard, 75013 Paris, France*
[b] *US Geological Survey, ms/470, 345 Middlefield Rd, Menlo Park, CA 94025, United States*
[c] *Centro Nacional de Investigación sobre la Evolución Humana (CENIEH) Paseo Sierra de Atapuerca s/n, 09002 Burgos, Spain*
[d] *Institut Català de Paleoecologia Humana i Evolució Social, C/Marcel·lí Domingo s/n (Edifici W3), Campus Sescelades, 43007 Tarragona, Spain*
[e] *Àrea de Prehistòria, Dept. d'Història i Història de l'Art, Univ. Rovira i Virgili, Fac. de Lletres, Av. Catalunya, 35, 43002 Tarragona, Spain*
[f] *Laboratoire des Sciences du Climat et de l'Environnement, Avenue de la Terrasse, 91198 Gif-sur-Yvette Cedex, France*
[g] *GEOTOP, Université de Québec à Montréal, Montréal, Québec H3C 3P8, Canada*
[h] *CEA/I²BM, F-91401 Orsay Cedex, France*
[i] *Institute of Vertebrate Paleontology and Paleoanthropology of Beijing (IVPP), Beijing, China*
[j] *Centro Mixto UCM-ISCIII de Evolución y Comportamiento Humanos Instituto de Salud Carlos III, C/Sinesio Delgado 4, Pabellón 14, 28029 Madrid, Spain*

ARTICLE INFO

Article history:
Received 28 January 2013
Accepted 9 May 2013
Available online xxx

Keywords:
Middle Pleistocene
Eurasia
Gran Dolina
Luminescence
Bayesian analysis
Homo antecessor

ABSTRACT

The Sierra de Atapuerca, northern Spain, is known from many prehistoric and palaeontological sites documenting human prehistory in Europe. Three major sites, Gran Dolina, Galería and Sima del Elefante, range in age from the oldest hominin of Western Europe dated to 1.1 to 1.3 Ma (millions of years ago) at Sima del Elefante to c.a. 0.2 Ma on the top of the Galería archaeological sequence. Recently, a chronology based on luminescence methods (Thermoluminescence [TL] and Infrared Stimulated Luminescence [IRSL]) applied to cave sediments was published for the Gran Dolina and Galería sites. The authors proposed for Galería an age of 450 ka (thousands of years ago) for the units lower GIII and GII, suggesting that the human occupation there is younger than the hominid remains of Sima de los Huesos (>530 ka) around 1 km away.

In this paper, we present new results obtained by combined Electron Spin Resonance/Uranium-series (ESR/U-series) dating on 20 herbivorous teeth from different levels at the Galería site. They are in agreement with the TL results for the upper part of the stratigraphic sequence (GIV and GIIIb), in the range of between 200 and 250 ka. But for the GIIIa to GIIb levels, the TL ages become abruptly older by 200 ka while ESR ages remain relatively constant. Finally, the TL and ESR data agree in the lowest part of the section (GIIa); both fall in the range of around 350–450 ka. Our results suggest a different interpretation for the GII, GIII and GIV units of Galería and the upper part of Gran Dolina (TD10 and TD11) than obtained by TL. The ESR/U-series results are supported by a Bayesian analysis, which allows a better integration between stratigraphic information and radiometric data.

Introduction

The Sierra de Atapuerca, located in northern Spain (Fig. 1a), has provided an incredible amount of palaeontological and archaeological data documenting human prehistory in Europe during the last million years (Rodríguez et al., 2011). Structurally, the Sierra de Atapuerca is an overturned anticline with a NE vergency and Iberian NNW–SSE direction (Pineda and Arce, 1997). Recent investigations combining geomorphological evolution analyses of the

* Corresponding author.
E-mail addresses: falguere@mnhn.fr (C. Falguères), bahain@mnhn.fr (J.-J. Bahain), jbischoff@usgs.gov (J.L. Bischoff), alfredo.perez@cenieh.es (A. Pérez-González), anaisabel.ortega@cenieh.es (A.I. Ortega), aolle@iphes.cat (A. Ollé), anita.quiles@lsce.ipsl.fr (A. Quiles), ghaleb.bassam@uqam.ca (B. Ghaleb), moreno@mnhn.fr (D. Moreno), jean-michel.dolo@cea.fr (J.-M. Dolo), shao@mnhn.fr (Q. Shao), jvallverdu@iphes.cat (J. Vallverdú), ecarbonell@iphes.cat (E. Carbonell), josemaria.bermudezdecastro@cenieh.es (J.M. Bermúdez de Castro), jlarsuaga@isciii.es (J.L. Arsuaga).

0047-2484/$ – see front matter © 2013 Elsevier Ltd. All rights reserved.
http://dx.doi.org/10.1016/j.jhevol.2013.05.005

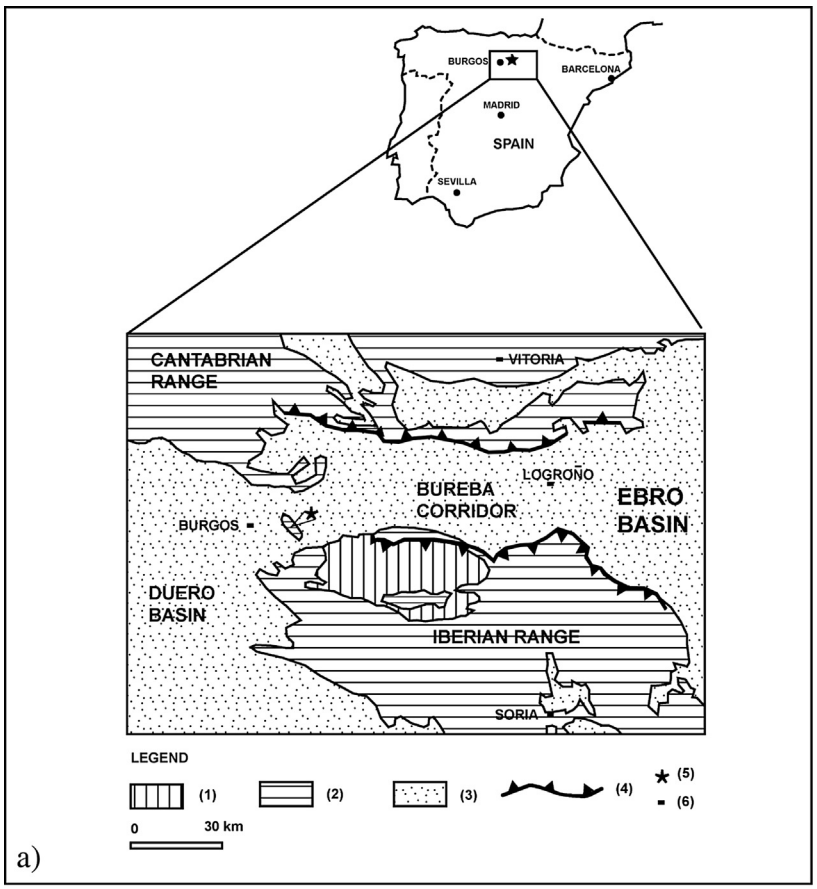

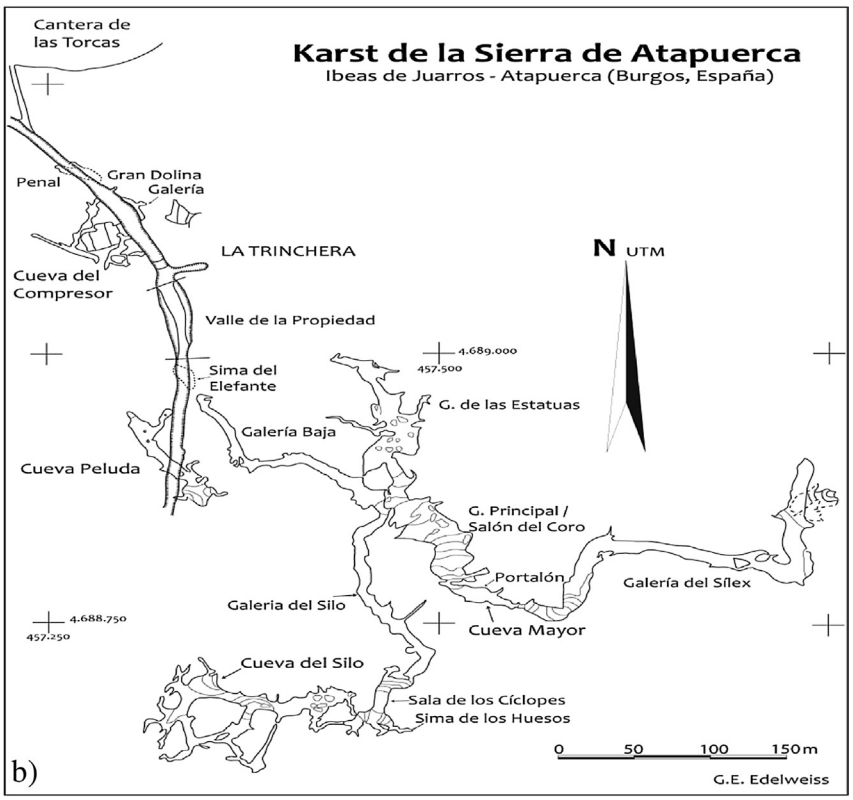

Figure 1. a) General geological context of the Sierra de Atapuerca (Burgos). Caption: (1) Palaeozoic; (2) Mesozoic; (3) Cenozoic; (4) Overthrust; (5) Site; (6) Cities. b) Location of main prehistorical sites in the Trinchera del Ferrocarril.

Please cite this article in press as: Falguères, C., et al., Combined ESR/U-series chronology of Acheulian hominid-bearing layers at Trinchera Galería site, Atapuerca, Spain, Journal of Human Evolution (2013), http://dx.doi.org/10.1016/j.jhevol.2013.05.005

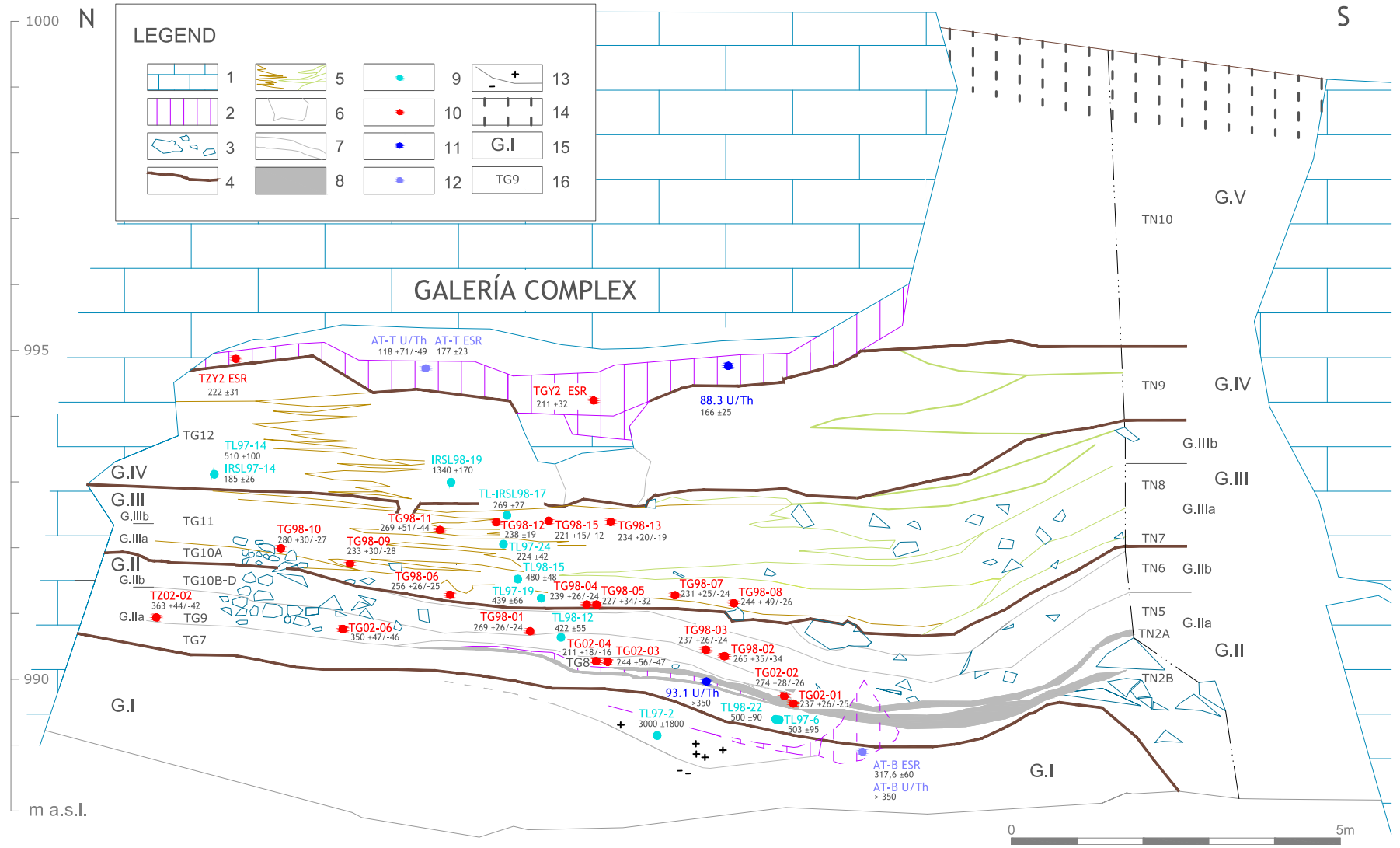

Figure 2. Stratigraphic scheme of the cave deposits at Galería Complex, with location of samples of luminescence, ESR and U-series. Caption: 1) Upper Cretaceous limestone and dolomite (wall of Galería Complex); 2) Speleothems; 3) Limestone blocks and cobbles; 4) Main stratigraphic unconformities; 5) Lateral facies variations from clay loam to gravel (on the left part) and from gravels to breccia (on the right part); 6) Cut and fill; 7) Limit of GII unit layers; 8) Bat guano level; 9) Luminescence samples (Berger et al., 2008); 10) ESR samples (Falguères, 1986; this work); 11) U/Th sample (Bischoff, Unpublished data); 12) U/Th and ESR samples (Grün and Aguirre, 1987); 13) Matuyama-Brunhes reversal (Pérez-González et al., 1999); 14) Soil; 15) Allostratigraphic units; 16) Archaeo-palaeontological levels.

Sierra de Atapuerca landscape (Benito-Calvo, 2004) and the study of the karst systems (Ortega et al., 2012) revealed a connection between the karst formation and the evolution of the nearby Arlanzón river. Electron Spin Resonance (ESR) results obtained on the alluvial terraces of this valley (Moreno et al., 2012) are consistent and reinforce the chronostratigraphic framework established previously by the combination of geomorphologic and palaeomagnetic data (Benito-Calvo et al., 2008). The Atapuerca caves consist of multilevel systems of inactive subhorizontal passages perched about 90, 70 and 60 m above the current course of the Arlanzón river (Ortega et al., 2012). The passages communicate by rooms, chimneys and pipes. Important collapses caused the appearance of wide rooms and sinks filled with allochtonous materials in which faunal remains and lithic artefacts are associated.

Three major sites were discovered when a railway trench (Trinchera del Ferrocarril) was cut at the beginning of the twentieth century, exposing the Gran Dolina, Galería and Sima del Elefante karst infillings, which document the entire Pleistocene (Fig. 1b). The oldest archaeological sequence is represented by Sima del Elefante, which has produced a number of lithic tools of Mode 1 technology associated with a fragmentary human mandible, a phalanx and fragmentary humerus, found in the lowermost levels (TE9) of the stratigraphic sequence (Bermúdez de Castro et al., 2011). This unit is of reversed magnetic polarity. Based on the faunal assemblage and cosmogenic Be/Al dates, this reversed polarity has been interpreted as the Matuyama chron (Parés et al., 2006; Carbonell et al., 2008). The uppermost levels (TE17-TE19), exhibiting a normal polarity, could belong either to the Jaramillo subchron or to the Brunhes chron. The TE8-TE16 levels could be coeval with the lowermost units of the Gran Dolina site located at the northern part of the Trinchera. Human remains associated with primitive lithic tools (Carbonell et al., 1999a) and a rich fauna characteristic of an Early Pleistocene age (Cuenca-Bescós et al., 1999) were found in a well constrained stratigraphic context at Gran Dolina (Parés and Pérez-Gonzalez, 1995; Falguères et al., 1999). The fossil hominids have been proposed as a new species, *Homo antecessor*, a possible common ancestor of modern humans and Neanderthals (Bermúdez de Castro et al., 1997). However, some authors currently working on the origin of *Homo heidelbergensis* question that *H. antecessor* might be its ancestor (Stringer, 2012).

The Galería complex is less than 100 m from Gran Dolina (Fig. 1b). Both correspond to a cave entrance, totally filled by the intermediate level of the karst system (Ortega et al., 2012). Galería was excavated between 1979 and 1995 on a 35 square metre surface. It is a typical sediment infilling where faunal remains and lithic artefacts were discovered in a well-established stratigraphic context (Pérez-González et al., 1999; Carbonell et al., 1999b). Several levels yielded a number of lithic tools of Mode 2 technology that are also present, rarely, in the uppermost levels of Gran Dolina and Sima de los Huesos (Ollé et al., 2013). Sima de los Huesos, not exposed to the outside, contains the skeletal remains of at least 28 individuals in a Middle Pleistocene mud-breccia with a single Mode 2 handaxe (Carbonell et al., 2003; Bermúdez de Castro et al., 2004).

The Spanish team decided to open new excavations at Galería since 2011 and at Covacha de los Zarpazos from 2002 to 2010. In order to establish a chronological framework for Galería, we analyzed a number of ungulate teeth unearthed from the fossiliferous levels by both ESR and Uranium-series (U-series) methods. We compare our new results with those obtained by luminescence at Galería and Gran Dolina (upper levels) (Berger et al., 2008) and by U-series at Sima de los Huesos (Bischoff et al., 1997, 2007).

A Bayesian analysis of the dating results provides a more constrained chronology for Galería. This approach was applied to analyze the age differences between the two dating methods on GIII and GIIa levels.

Stratigraphy

The Galería complex is cut longitudinally by the Trinchera. It contains three sub-sections: Tres Simas on the southern part, Galería, which is the main horizontal conduit, and Covacha de los Zarpazos, located in the northern part. These sections likely represent a huge room supplied by a common conduit (Ortega, 2009).

Five infilling phases form the stratigraphic sequence of Galería (Pérez-González et al., 1995) named from the bottom to the top, GI to GV units (Fig. 2).

Unit GI constitutes a 5 m thick endokarstic sedimentary facies that is archaeologically sterile. In this unit is observed a reversed magnetostratigraphic polarity attributed to the Matuyama/Brunhes boundary, suggesting a great antiquity for these levels (Pérez-González et al., 1999).

In the uppermost stratigraphic units (GII to GIV), a rich assemblage of lithic artefacts associated with faunal remains were found. Unit GII is the first unit constituted by allochtonous sediments and was deposited with an erosive and angular unconformity on GI. GII consists of gravely clastic facies containing fallen blocks and is enveloped in a silty-clayey matrix. The sediments are allochtonous. The base of the unit contains a guano deposit interstratified with black clays. This guano level reaches 20–30 cm thick in the southern and central part of the infilling. This phenomenon led to post-depositional phosphated aluminium hydroxide, which altered the bones. In situ lixivation, attested by weathering rings in limestone and depleted calcitic sands and silt, suggest bone destruction too (Vallverdu, 1999). In 1976, a human mandibular fragment was found during the first excavations of Galería. Though its exact stratigraphic location was unknown, it was attributed to Unit GII (Rosas and Bermúdez de Castro, 1999).

Unit GIII lies also in angular unconformity on GII. GIII is constituted only of clastic sediments with a heterogeneous size distribution in which lateral facies variations can be observed. Towards the northern part of the sequence, gravity deposits are interstratified with well organized facies deposited by flood water. GIII has been sub-divided into GIIIa and GIIIb according to the sedimentation texture and archaeological records. A cranial human fragment, discovered at the entrance of the Zarpazos, was stratigraphically attributed to the base of GIII unit (Arsuaga et al., 1999).

Unit GIV is similar to the GIII with a thickness of between 1.5 and 2 m.

Unit GV corresponds to a vertical infilling reaching a thickness of 5 m and represents the last clogging of the cavity (Pérez-González et al., 2001).

Previous radiometric results

Because of the importance of the recent discoveries and of the richness of the Atapuerca archaeological sequences, a number of

Table 1
Non-destructive gamma-ray spectrometric dating of AT76 mandible from Galería, Atapuerca, Spain.

	AT76 mandible
Mass (g)	8.85
U content (ppm)	54 ± 3
U^{234}/U^{238}	1.704 ± 0.215
Th^{230}/U^{234}	0.569 ± 0.077
Pa^{231}/U^{235}	0.952 ± 0.030
Th^{230}/Th^{232}	37 ± 4
U–Th Age (ka)	85 + 19/−16
U–Pa Age (ka)	144 + 46/−23

Please cite this article in press as: Falguères, C., et al., Combined ESR/U-series chronology of Acheulian hominid-bearing layers at Trinchera Galería site, Atapuerca, Spain, Journal of Human Evolution (2013), http://dx.doi.org/10.1016/j.jhevol.2013.05.005

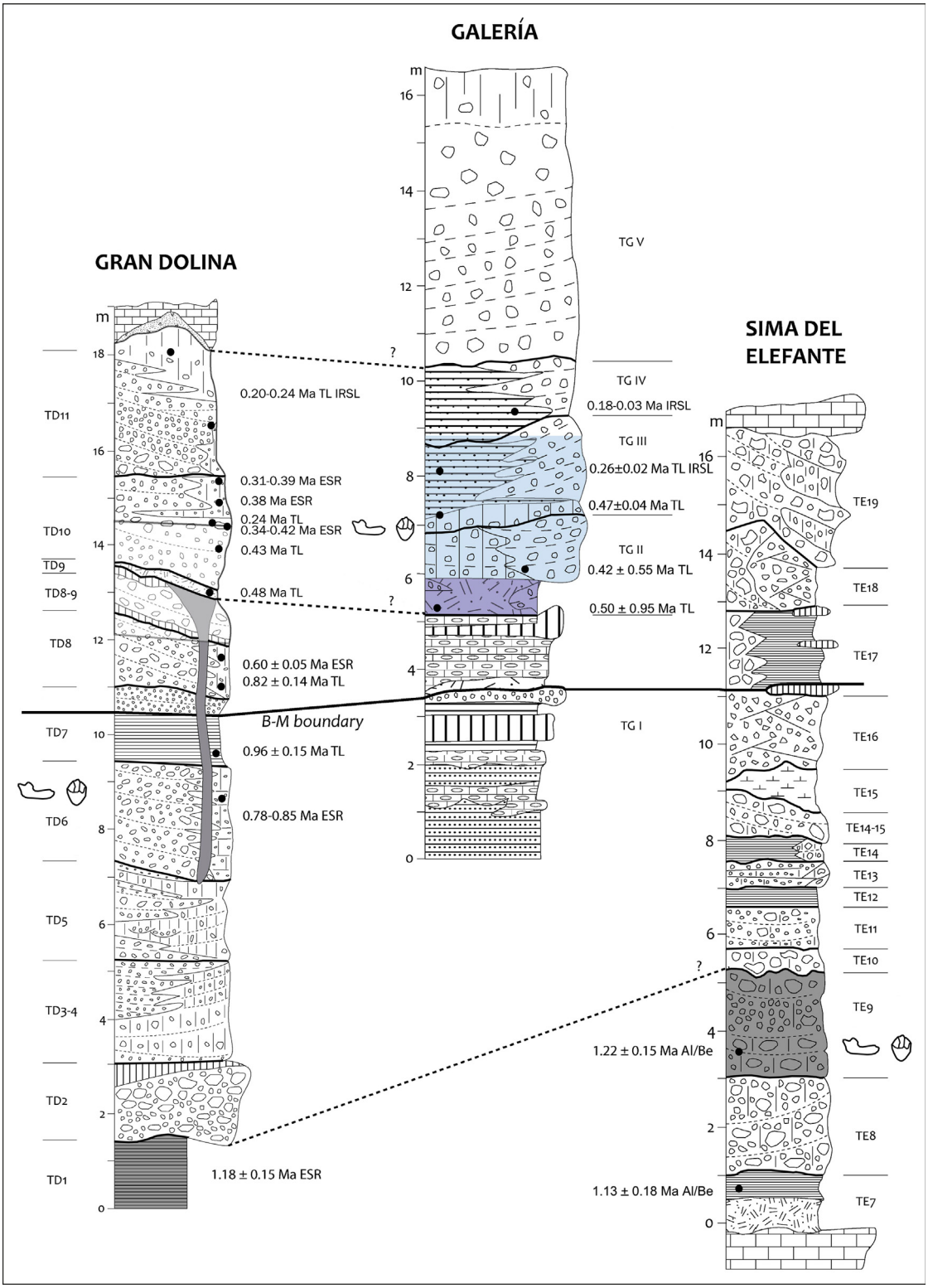

Figure 3. Main geochronological guidemarks of the three infilling of Trinchera before this work. A palaeomagnetic reversal attributed to Matuyama-Brunhes boundary is observed in the three sequences (Dolina: Parés and Pérez-González, 1995; Galería: Pérez-González et al., 1999; Elefante: Parés et al., 2006). Cosmogenic burial dates of 1.22 Ma are provided for the human remains in the TE9 layer of Elefante (Carbonell et al., 2008) and could be coeval with the basis of Dolina layers dated by ESR-OB to about 1.10–1.30 Ma (Moreno et al., in prep.). For Dolina, the other dates are published in Berger et al. (2008) for TL/IRSL data and in Falguères et al. (1999) for ESR-US data on teeth.

Please cite this article in press as: Falguères, C., et al., Combined ESR/U-series chronology of Acheulian hominid-bearing layers at Trinchera Galería site, Atapuerca, Spain, Journal of Human Evolution (2013), http://dx.doi.org/10.1016/j.jhevol.2013.05.005

dating methods have been applied. Although the chronological framework of Sima del Elefante and Gran Dolina is primarily based on biostratigraphy and palaeomagnetism, some radiometric data have reinforced the chronostratigraphy. At Sima del Elefante, cosmogenic nuclides provided an age ranging between 1.3 and 1.1 Ma (millions of years ago) for the TE9 layer in which a hominid mandibular fragment was found in 2007 (Carbonell et al., 2008). This result is in agreement with palaeomagnetic data suggesting that the Matuyama/Brunhes boundary is recorded in upper levels, TE16.

In 2008, a number of luminescence analyses performed on the Galería and Gran Dolina stratigraphical sequences were published by Berger et al. (2008). The results based on Infra-Red Stimulated Luminescence (IRSL) and on Thermoluminescence (TL) analyses constrasted with earlier data obtained at Gran Dolina, particularly with the ESR/U-series dates on teeth and palaeomagnetism (Falguères et al., 1999; Parés and Pérez-González, 1999). The luminescence results will be discussed further and compared with the ages obtained in this study.

A direct, non-destructive gamma-ray analysis on the human mandible fragment (AT76) from unit GIII yielded ages of 85 + 19/−16 ka (thousands of years ago) and 144 + 46/−23 ka by U/Th and U/Pa, respectively (Yokoyama, Unpublished data). This is in contradiction with an age older than 250 ka based on stratigraphic correlation (Rosas and Bermúdez de Castro, 1999). The inconsistent U/Th and U/Pa results indicate a post-depositional uranium uptake into the mandible resulting in apparent age underestimations (Table 1).

Speleothems were also dated in Galería. The upper stalagmitic floor, which covers the GIV unit, yielded alpha spectrometry U-series dates with a mean age of 166 ± 25 ka (Bischoff, Unpublished data) in agreement with another U/Th date of 177 ± 23 ka by Grün and Aguirre (1987). Three calcite samples were dated by ESR methods (Falguères, 1986): one from the same level provided an age of 212 ± 32 ka; another from the upper part of the infilling of Covacha de los Zarpazos, yielded an age of 222 ± 31 ka. These analyses indicated that the GV unit was deposited before the end of MIS7. A third ESR sample from the upper part of stalagmitic floor located in Tres Simas (TS-S), in the southern part of Galería section, yielded an age of 256 ± 33 ka. All of these calcitic samples contain very low uranium content, less than 0.1 ppm.

Two calcitic samples from the lowermost stalagmitic crust of GI unit, provided an age of 317 ± 60 ka and >350 ka (Grün and Aguirre, 1987). Another sample, at the bottom of GII unit (TG8) has also yielded an age older than 350 ka (Bischoff, Unpublished data).

Fig. 3 shows the three composite sections of Sima del Elefante, Gran Dolina and Galería including the main geochronological results.

Material and methods

The combined ESR/U-series (ESR-US) model takes into account both ESR and U-series data, and including radioelement contents, isotopic ratios, palaeodoses and external gamma-dose rate, allows the reconstruction of the uranium uptake history in each dental tissue using a specific U-uptake parameter (*p*-value) (Grün et al., 1988). The model cannot account for uranium loss. The relevance of the method was discussed in Grün (2009a). The application of this combined approach allows the dating of the whole Middle Pleistocene period (Bahain et al., 2007; Falguères et al., 2010).

Sample selection and preparation

Twenty herbivorous teeth from the GII and GIII units (Fig. 2) were selected and prepared in the laboratory for analyses. Enamel, dentine and cementum were separated mechanically and their radioisotope contents measured by TIMS for enamel (Geological Survey, Menlo Park, USA) and alpha-ray spectrometry for dentine and cementum (MNHN, Paris), using standard methods (Bischoff et al., 1988), and gamma-ray spectrometry (Yokoyama and Nguyen, 1980).

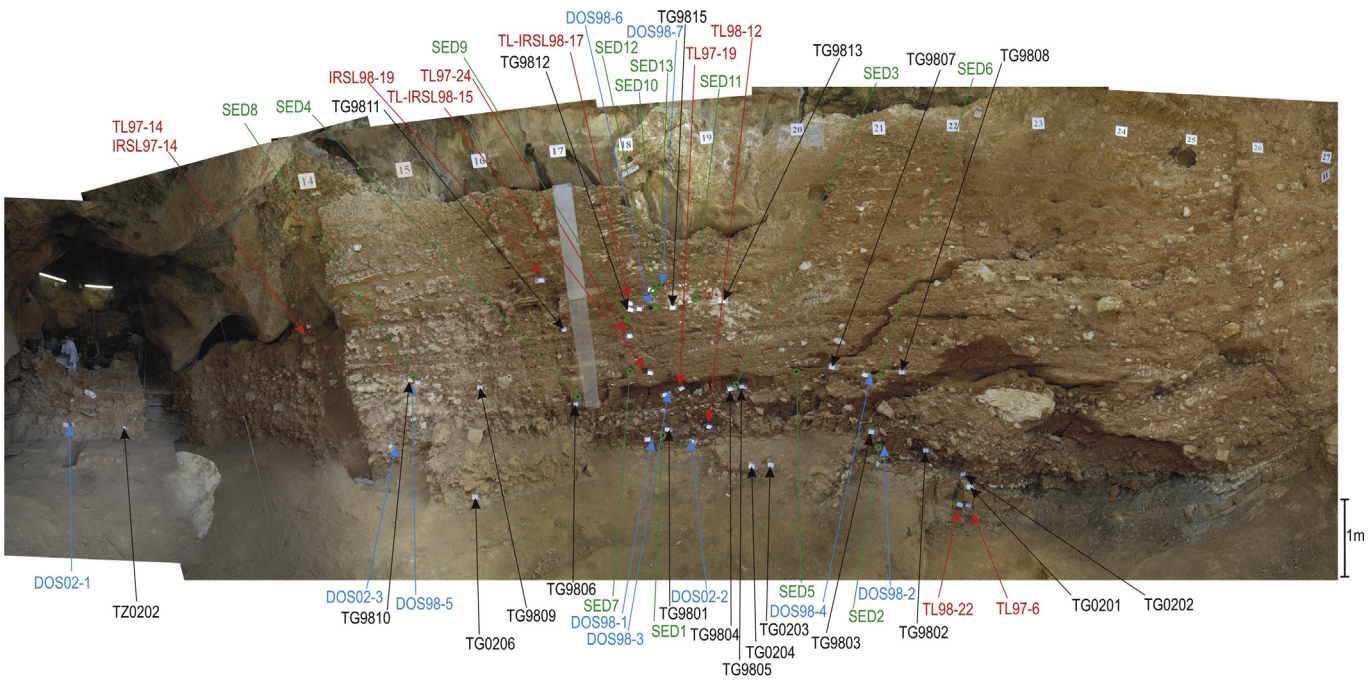

Figure 4. Location of the analyzed ESR-US samples (black), sediments (green) dosimeters (blue) used for ESR calculations, and luminescence samples (red) analyzed in Berger et al. (2008) at Galería Complex. (For interpretation of the references to colour in this figure legend, the reader is referred to the web version of this article.)

Please cite this article in press as: Falguères, C., et al., Combined ESR/U-series chronology of Acheulian hominid-bearing layers at Trinchera Galería site, Atapuerca, Spain, Journal of Human Evolution (2013), http://dx.doi.org/10.1016/j.jhevol.2013.05.005

A part of the enamel, after cleaning of its surface on both sides (inner and outer sides) to eliminate the effect of external alpha radiation, was ground, sieved and the 100–200 μm fraction split into ten aliquots. Nine of the ten were irradiated with a calibrated ^{60}Co gamma-ray source from 200 to 8000 Gy.

Measurements

ESR measurements were performed at room temperature on an EMX-6 Bruker spectrometer (X band, 9.82 GHz) with a microwave power of 10 mW and a modulation amplitude of 0.1 mT. A scan range of 10 mT and a scan time of 4 min with a modulation frequency of 100 kHz was used for each spectrum. Each ESR measurement was repeated three times for each dose. The equivalent doses (D_E) were determined from the asymmetric enamel T1-B2 signal at $g = 2.0018$ (Grün et al., 2008) by fitting a single exponential function (SSE) (Yokoyama et al., 1985). ESR age calculations were carried out with the ESR-DATA program of Grün (2009b), which uses an alpha efficiency of 0.13 ± 0.02 (Grün and Katzenberger-Apel, 1994) and Monte-Carlo beta attenuation

Table 2
ESR and U-series data on fossil herbivorous teeth from Galería site.

Sample	Species	Tissue	U (ppm)	^{234}U/^{238}U	^{230}Th/^{234}U	^{222}Rn/^{230}Th	T enamel (μm)	Removed enamel[a] (μm)	DE (Gy)
GIIIb									
		D	39.05	1.374 ± 0.026	0.677 ± 0.022	0.26			
TG9815	*Equus* (deciduous incisor)	E	0.84	1.510 ± 0.104	0.864 ± 0.059	0.58	1140	80; 40	481.1 ± 11.7
		D	42.93	1.280 ± 0.029	0.565 ± 0.019	0.29			
TG9813	*Equus* (deciduous incisor)	E	2.66	1.764 ± 0.086	0.689 ± 0.034	0.54	1320	50; 150	525.5 ± 14.4
		D	41.52	1.474 ± 0.029	0.771 ± 0.019	0.28			
TG9812	*Equus* (deciduous incisor)	E	1.43	1.450 ± 0.026	0.828 ± 0.026	0.20	1120	80; 100	524.6 ± 27.4
		D	33.06	1.289 ± 0.029	0.817 ± 0.024	0.35			
TG9811	*Equus* (deciduous)	E	5.46	1.350 ± 0.027	0.908 ± 0.049	0.28	1140	150; 70	606.1 ± 31.0
		C	30.12	1.386 ± 0.029	0.907 ± 0.023	0.24			
GIIIa									
		D	27.62	1.409 ± 0.036	0.776 ± 0.023	0.34			
TG9810	*Equus* (P3/4)	E	2.03	1.450 ± 0.024	0.735 ± 0.015	0.42	1350	110; 120	389.5 ± 14.1
		C	30.53	1.437 ± 0.026	0.688 ± 0.017	0.29			
		D	31.99	1.409 ± 0.029	0.796 ± 0.022	0.29			
TG9809	*Equus* (deciduous)	E	5.97	1.390 ± 0.031	0.729 ± 0.012	0.35	940	70; 90	628.3 ± 30.3
		C	35.79	1.371 ± 0.026	0.781 ± 0.019	0.29			
		D	40.39	1.438 ± 0.029	0.935 ± 0.025	0.24			
TG9808	*Equus* (molar)	E	3.60	1.430 ± 0.030	*1.330 ± 0.072*	0.35	1350	100; 130	550.6 ± 12.3
		C	34.02	1.594 ± 0.034	0.887 ± 0.022	0.22			
		D	41.00	1.361 ± 0.028	0.786 ± 0.022	0.30			
TG9807	*Equus* (molar)	E	1.23	1.410 ± 0.026	0.786 ± 0.026	0.70	1620	240; 140	487.9 ± 30.5
		C	37.04	1.372 ± 0.023	0.815 ± 0.019	0.25			
		D	51.00	1.493 ± 0.027	0.791 ± 0.019	0.30			
TG9806	*Equus* (incisor)	E	1.51	1.540 ± 0.023	*1.020 ± 0.034*	0.40	1640	190; 180	506.1 ± 32.7
		D	35.90	1.342 ± 0.031	0.885 ± 0.028	0.20			
TG9805	*Equus* (P3/4)	E	3.35	1.390 ± 0.021	0.789 ± 0.025	0.37	1580	110; 240	494.5 ± 44.2
		C	33.73	1.333 ± 0.025	0.714 ± 0.019	0.26			
		D	35.81	1.505 ± 0.024	0.856 ± 0.023	0.26			
TG9804	*Equus* (P2)	E	2.24	1.450 ± 0.023	0.804 ± 0.022	0.64	1680	230; 220	494.5 ± 22.7
		C	37.27	1.494 ± 0.025	0.835 ± 0.019	0.22			
GIIb									
		D	44.15	1.168 ± 0.023	0.691 ± 0.021	0.28			
TG9803	*Equus* (molar)	E	2.39	1.310 ± 0.028	0.662 ± 0.015	0.39	1290	120; 160	436.3 ± 20.5
		C	23.31	1.339 ± 0.036	0.812 ± 0.025	0.20			
		D	41.53	1.380 ± 0.029	0.896 ± 0.026	0.27			
TG9802	*Equus* (P3/4)	E	2.08	1.370 ± 0.023	0.778 ± 0.052	0.61	1060	60; 40	604.3 ± 46.9
		C	40.03	1.360 ± 0.026	0.886 ± 0.022	0.20			
		D	31.22	1.683 ± 0.022	0.845 ± 0.018	0.34			
TG9801	*Bison* (molar)	E	1.49	1.630 ± 0.027	0.828 ± 0.015	0.52	1360	70; 70	585.8 ± 28.6
GIIa									
		D	13.01	1.519 ± 0.037	0.729 ± 0.052	0.73			
TZ0202	Bovid (molar)	E	0.33	1.571 ± 0.098	0.824 ± 0.075	0.82	917	56; 20	648.3 ± 54.0
		D	26.76	1.408 ± 0. 026	0.846 ± 0.032	0.41			
TG0206	*Equus* (P3 deciduous)	E	2.77	1.442 ± 0.160	0.845 ± 0.088	0.38	1000	63; 149	824.2 ± 70.2
		D	46.05	1.309 ± 0.022	0.657 ± 0.024	0.56			
TG0204	*Equus* (incisor)	E	0.47	1.136 ± 0.100	0.966 ± 0.296	0.79	1330	122; 36	349.8 ± 8.0
		D	44.88	1.317 ± 0.017	0.831 ± 0.025	0.45			
TG0203	Bovid (molar)	E	4.92	1.399 ± 0.041	0.801 ± 0.034	0.31	1142	241; 200	554.3 ± 31.9
		D	31.63	1.152 ± 0.028	0.790 ± 0.039	0.47			
TG0202	*Equus* (P2)	E	0.64	1.058 ± 0.089	*1.221 ± 0.223*	1.00	1208	96; 73	483.6 ± 31.4
		C	20.48	1.262 ± 0.022	0.780 ± 0.029	0.35			
		D	17.57	1.349 ± 0.029	0.778 ± 0.029	0.46			
TG0201	Bovid (molar)	E	2.67	1.390 ± 0.057	0.873 ± 0.045	0.38	1066	112; 122	432.3 ± 19.1

E = enamel, *D* = dentine, C = cementum. Uncertainties for isotopic ratios are given with ±1 sigma.
The initial (T) and removed enamel thickness is used for the age calculation.
The results written in italics underline a geochemical problem, which could be due to a possible uranium leaching.
The U-series for enamel were done by TIMS in the USGS lab while the dentine and cementum U-series were performed in Paris Lab using alpha-ray spectrometry.
[a] The first number corresponds to the enamel subtracted in the dentine-enamel side; the second number to the cementum (sediment)-enamel side.

Please cite this article in press as: Falguères, C., et al., Combined ESR/U-series chronology of Acheulian hominid-bearing layers at Trinchera Galería site, Atapuerca, Spain, Journal of Human Evolution (2013), http://dx.doi.org/10.1016/j.jhevol.2013.05.005

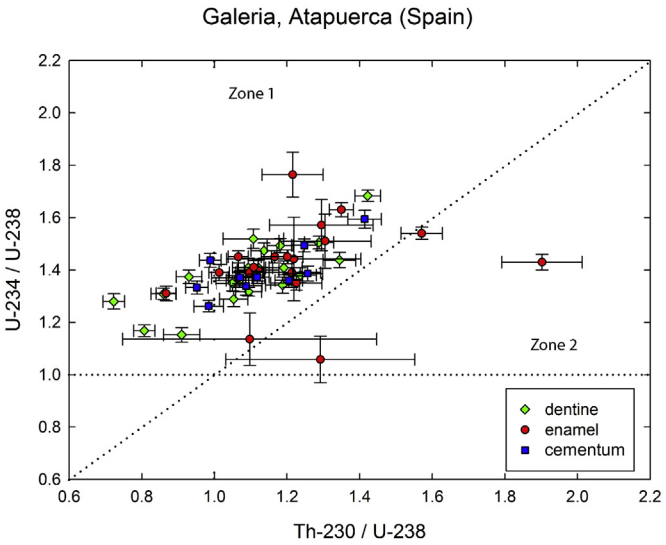

Figure 5. Theoretical evolution of the ^{238}U–^{234}U–^{230}Th disequilibria in the ($^{234}U/^{238}U$) versus ($^{230}Th/^{238}U$) activity ratio diagram for each dental tissue from Galería samples. All the samples are in the domain of reliability (Zone 1), close to the equiline, indicating thus a U-uptake process, which is not recent (i.e., p parameter which tend towards −1), except two of them that are located in the complex area (Zone 2).

factors (Marsh, 1999) based on the thickness of the tooth enamel and outer layers removed. In addition, the following parameters were used:

1) The water content was estimated to be 3 wt% in the enamel, 5 to 10 wt% in the dentine and in the cementum, and 12 to 20 wt% in the sediment.
2) Gamma-ray spectrometry was used to determine the sediment radioisotopes U, Th and K where the teeth were collected. The dose rate was calculated according to Adamiec and Aitken (1998). In addition, TL dosimeters were inserted in the layers and left in situ for nearly one year (Fig. 4).
3) The effect of Ra and Rn loss in each tissue was determined by combining alpha-ray and gamma-ray measurements (Bahain et al., 1992).

Results and discussion

Table 2 exhibits the isotopic data, initial and removed enamel thickness and D_E for the samples. The U content ranges between 0.3 and 6.0 ppm in the enamel and between 13 and 51 ppm in dentine and cementum tissues. Fig. 5 shows that isotopic ratios are extremely homogeneous and appear in the domain of reliability (Zone 1). Only two samples indicate obvious uranium leaching, which is documented by the fact that their $^{230}Th/^{238}U$ ratio is greater than their $^{234}U/^{238}U$ ratio (Zone 2 in Fig. 5) (see details in Osmond and Ivanovich, 1992; Chabaux et al., 2003).

ESR/US ages

Table 3 provides the details about the dose rate, *p*-values and ages for the analyzed teeth. In spite of the heterogeneity in the analytical results, the obtained ESR-US ages are remarkably homogeneous for GIIIb, GIIIa and GIIb sub-levels, ranging between 220 and 280 ka.

For GIIa, the ages do not increase in the same way as the depth except for two samples (TZ0202 and TG0206) providing dates of approximately 350 ka marking out the basis of the archaeological sediments of the Galería infilling.

The results on TG8 and TN2B samples are obviously too young without exhibiting more 'recent' uptake than the other samples

Table 3
Components of dose-rates for US model of teeth and sediment, and ESR-US age estimates with correspondent *p*-values for fossil teeth from Galería.

Teeth	Units	Layer	($\beta + \gamma$) sediment + cosmic (μGy/a)	Internal dose rate ($\alpha + \beta$) enamel (μGy/a)	β dose rate cementum (μGy/a)	Total dose rate (μGy/a)	p enamel	p dentine	p cementum	Age (ka)
	GIIIb									
TG9815		TG11/GSU3	1692	481	–	2173	−0.88 ± 0.13	−0.63 ± 0.24	–	221 + 15/−12
TG9813		TG11/GSU3	1534	713	–	2247	−0.34 ± 0.18	0.19 ± 0.19	–	234 + 20/−19
TG9812		TG11/GSU3	1669	540	–	2209	−0.76 ± 0.09	−0.61 ± 0.09	–	238 ± 19
TG9811		TG11/GSU4	650	1367	239	2256	−0.87 ± 0.17	−0.67 ± 0.15	−0.86 ± 0.11	269 + 51/−44
	GIIIa									
TG9810		GSU11A	776	490	111	1377	−0.33 ± 0.14	−0.48 ± 0.12	−0.13 ± 0.16	283 + 30/−27
TG9809		GSU12	1168	1272	260	2700	−0.52 ± 0.13	−0.71 ± 0.11	−0.67 ± 0.11	233 + 30/−28
TG9808		GSU12	738	1325	196	2259	−1[a]	−0.96 ± 0.06	−0.85 ± 0.07	244 + 29/−26
TG9807		GSU12	1460	481	174	2115	−0.69 ± 0.11	−0.70 ± 0.10	−0.77 ± 0.09	231 + 25/−24
TG9806		TG10a/TN7	1258	722	–	1980	−1[a]	−0.67 ± 0.07	–	256 + 26/−25
TG9805		TG10a/TN7	1164	914	102	2180	−0.71 ± 0.14	−0.93 ± 0.09	−0.51 ± 0.16	227 + 34/−32
TG9804		TG10a/TN7	1164	761	148	2073	−0.70 ± 0.10	−0.81 ± 0.08	−0.77 ± 0.08	239 + 26/−24
	GIIb									
TG9803		TG10d	1197	528	114	1839	−0.27 ± 0.16	−0.41 ± 0.14	−0.74 ± 0.11	237 + 26/−24
TG9802		TG10d	1197	797	313	2307	−0.56 ± 0.20	−0.86 ± 0.10	−0.84 ± 0.09	262 + 35/−34
TG9801		TG10d	1576	606	–	2182	−0.64 ± 0.09	−0.68 ± 0.08		269 + 26/−24
	GIIa									
TZ0202		GIId	1619	168	–	1787	−0.39 ± 0.31	−0.01 ± 0.30	–	363 + 44/−42
TG0206		TG9	1576	781	–	2357	−0.57 ± 0.37	−0.52 ± 0.15	–	350 + 47/−46
TG0201		TN2B	1405	587	–	1992	−0.82 ± 0.16	−0.73 ± 0.13	–	(217 + 31/−28)
TG0204		TG8	1414	243	–	1657	−0.95 ± 0.05	0.00 ± 0.00	–	(211 + 18/−16)
TG0203		TG8	1396	878	–	2274	−0.68 ± 0.20	−0.77 ± 0.17	–	(244 + 56/47)
TG0202		TG8	1239	407	123	1769	−1[a]	−0.70 ± 0.08	−0.64 ± 0.13	(274 + 28/−26)

External dose-rates correspond to both sediment dose and cosmic dose ($\beta + \gamma$). Two types of measurements have been performed. About 100 g of sediment including rock fragments when they are present, were measured at least ten months after it had been inserted in a box. Sediments have been sampled in the same square and at the same height as the teeth. TL dosimeters have been placed in different levels at the exact location of the analyzed sediments. For samples lacking cementum tissue, the enamel was directly in contact with the sediment. The case dentine-enamel-cementum was used for some equid teeth, the cementum layer was thick enough to prevent the enamel from sediment beta particles.

[a] *p*-value was limited to −1 according with isotopic ratios (see table 2) suggesting a leaching uranium.

Please cite this article in press as: Falguères, C., et al., Combined ESR/U-series chronology of Acheulian hominid-bearing layers at Trinchera Galería site, Atapuerca, Spain, Journal of Human Evolution (2013), http://dx.doi.org/10.1016/j.jhevol.2013.05.005

(p-values range between 0 and −1). This suggests a complex geochemical history of these samples. TG0202 has an enamel p-value limited to −1 (when we take into account the positive error) and also exhibits a $^{230}Th/^{234}U$ ratio of 1.2, suggesting uranium leaching and the proposed age corresponds to a minimum age. TG0204 has a large error range on the isotopic ratios. The lower D_E values suggest also that the leaching occurred early after burial.

The dose rate measurements are difficult for the TG0201 to TG0204 samples and possibly can be overestimated, rendering the ages younger than the actual ages.

Biostratigraphy

The Carnivora found in the GII-GIII units are similar to many European Middle Pleistocene sites but lacks hyaenas like those found in TD8. Moreover, the absence of *Panthera gombaszoegensis* suggests that the layers are younger than TD8 (García et al., 1997; García, 2003).

The rodents of GII-GIII and their evolutionary stage suggest a good correlation with other Spanish Middle Pleistocene sites such as Áridos I, Ambrona and maybe a little bit younger than Arago. Remains of *Hystrix*, associated with Mediterranean species such as*Iberomys brecciensis* and *Arvicola*, and *Pliomys lenki*, suggest a temperate-warm climate, typical of an interglacial period (Cuenca-Bescós et al., 1999). Recently, faunal units or biozones (FU) have been proposed to classify the faunal successions and micro-vertebrates recorded in six karstic cavities of the Sierra de Atapuerca (Cuenca-Bescós et al., 2010). The GII and GIII units were placed in FU 6, a biozone defined by the appearance of *Iberomys brecciensis* and *Terricola atapuerquensis* and indicating an age between 0.78 and 0.10 Ma. At Atapuerca, the first appearance of *Arvicola* was observed at the bottom of TD10, which can be correlated with European Middle Acheulian sites such as Orgnac 3 and Aides.

Comparison with TL ages

Fig. 6 shows the earlier luminescence dates along with ESR-US ages of the present study. There is a good agreement from GIV to the base of GIIIb.

For the lower part of GIII unit (GIIIa), a sharp discrepancy appears in which the TL dates are 200 ka older than the ESR dates.

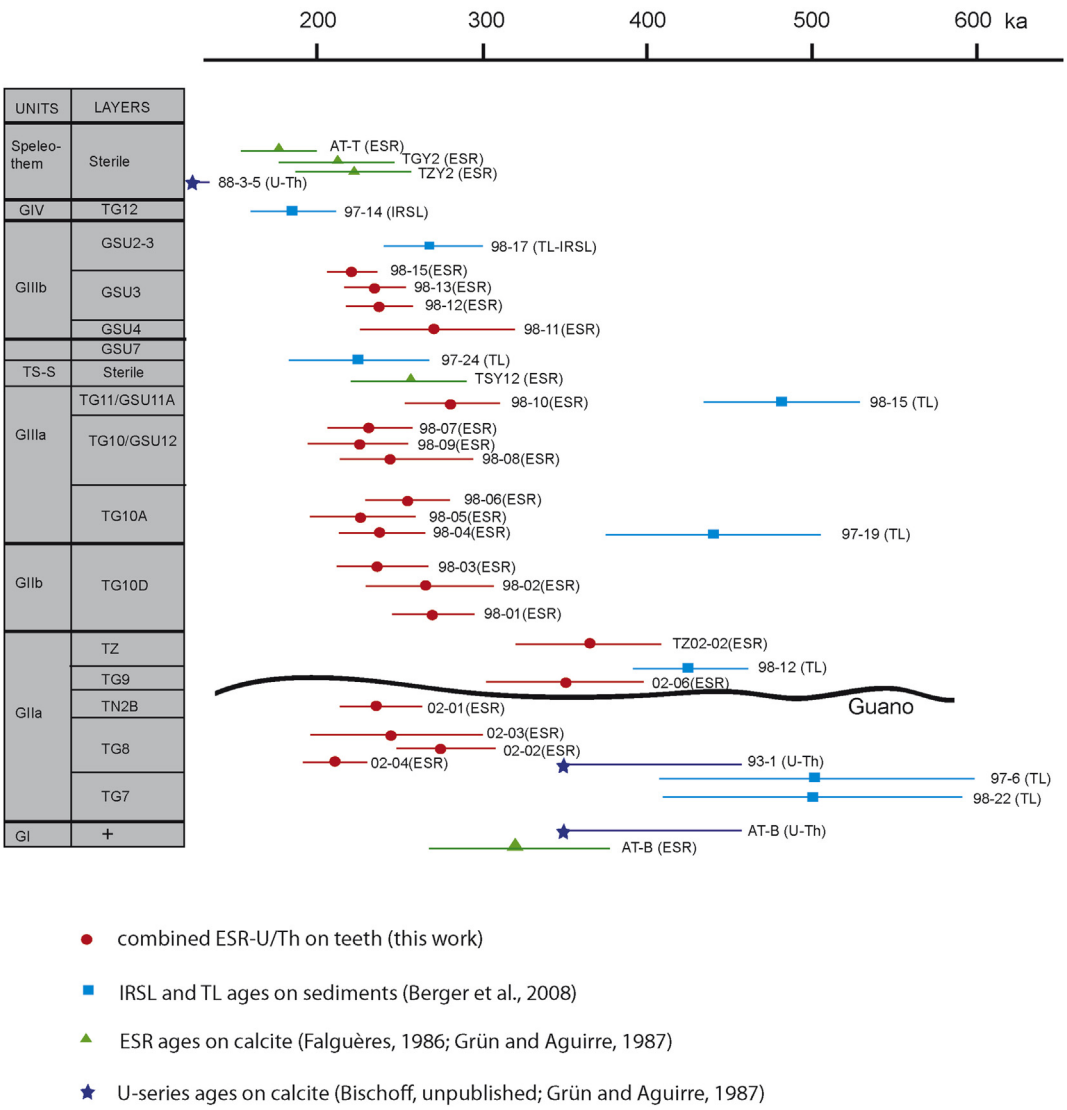

Figure 6. Radiometric ages of Galería section obtained by different dating methods. The sample TSY12 was taken in the southern part of Galería Complex called Tres Simas (TS-S), which can be attributed to a level equivalent to the lower part of GIIIb.

Please cite this article in press as: Falguères, C., et al., Combined ESR/U-series chronology of Acheulian hominid-bearing layers at Trinchera Galería site, Atapuerca, Spain, Journal of Human Evolution (2013), http://dx.doi.org/10.1016/j.jhevol.2013.05.005

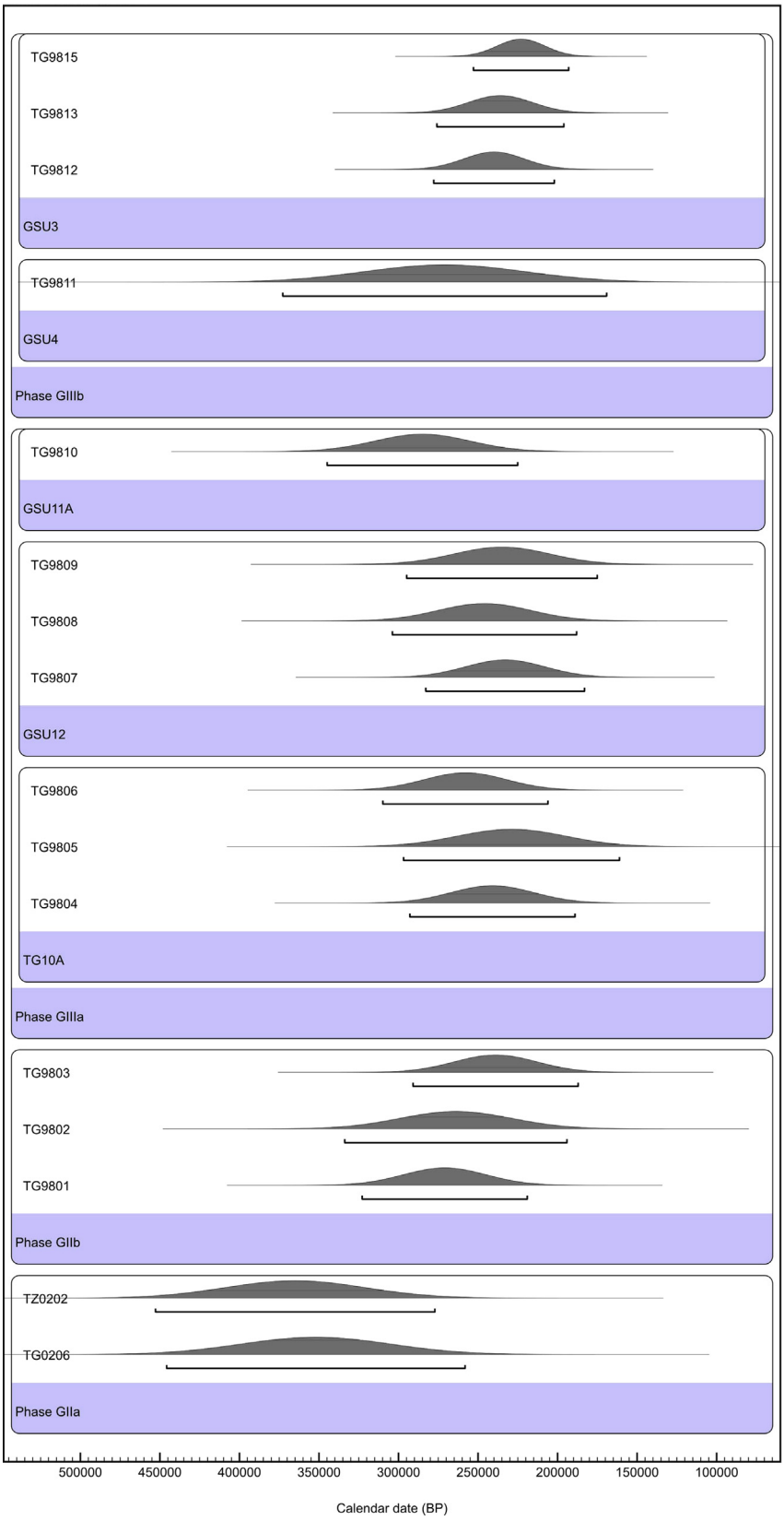

Figure 7. ESR-US dates on teeth organized by units deduced from the stratigraphic context. No constraint is applied on the probability densities. TG0201 and TG0204 outlier samples are excluded from the analysis (16 samples).

Please cite this article in press as: Falguères, C., et al., Combined ESR/U-series chronology of Acheulian hominid-bearing layers at Trinchera Galería site, Atapuerca, Spain, Journal of Human Evolution (2013), http://dx.doi.org/10.1016/j.jhevol.2013.05.005

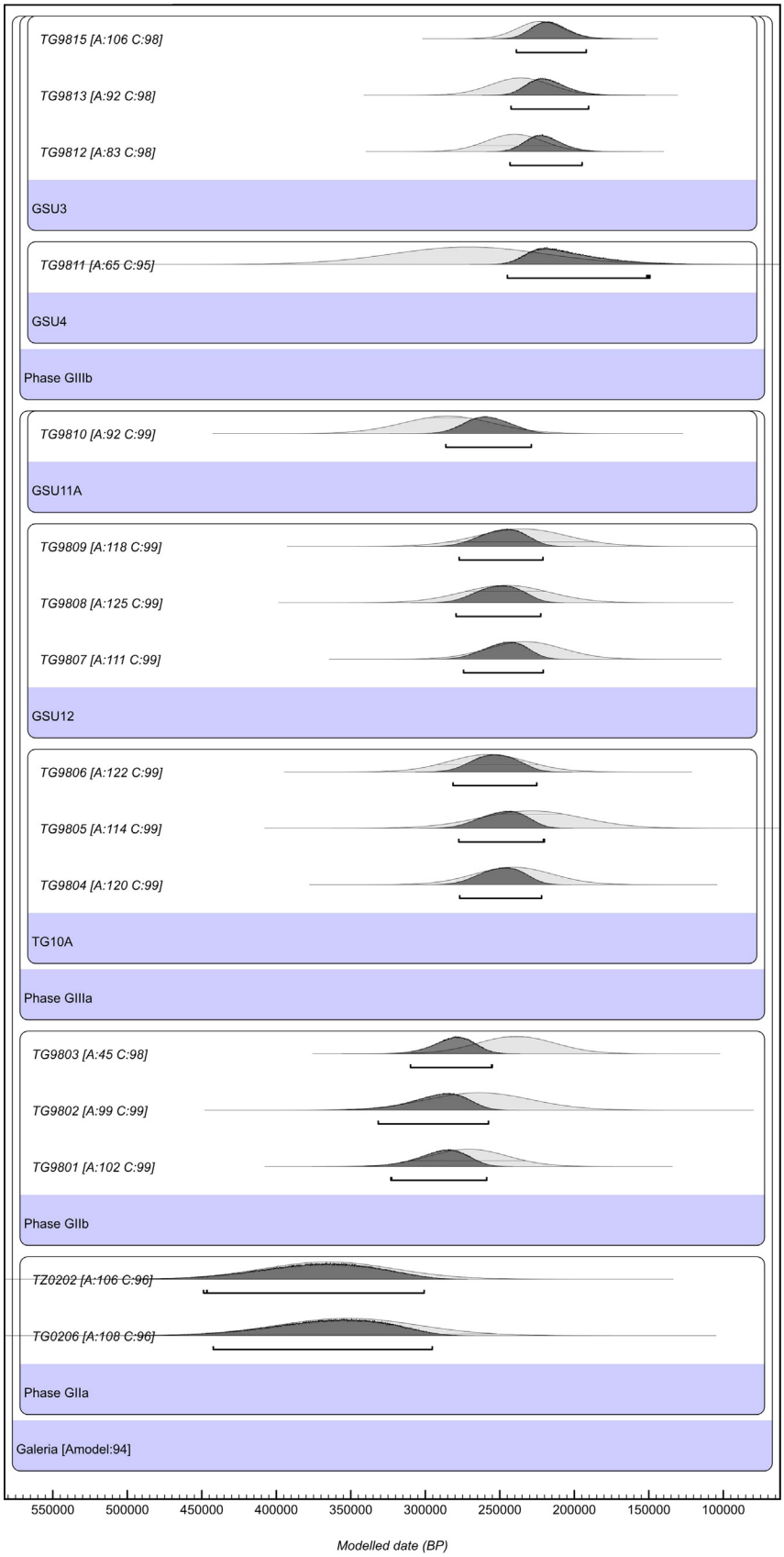

Figure 8. Bayesian modelling of the ESR-US dates on teeth. Probability densities are sequenced according to the stratigraphic context (OxCal4.1). A posteriori densities (deduced from the modelling) are shown in darker shade; the likelihoods (distribution laws deduced from the measurements, without any modelling) in lighter shade. This model is accepted with an agreement of 94 (Amodel = 94): ESR-US dates and stratigraphic context concur.

Please cite this article in press as: Falguères, C., et al., Combined ESR/U-series chronology of Acheulian hominid-bearing layers at Trinchera Galería site, Atapuerca, Spain, Journal of Human Evolution (2013), http://dx.doi.org/10.1016/j.jhevol.2013.05.005

There is no significant evidence of a stratigraphic discontinuity at this level. An initial explanation could be the fact that the TL dates, which have been determined from clayey sediment, are younger (TL9724) than those performed in the gravel matrix referred to as 'paella' (TL9815, TL9719). This phenomenon could be due to a difficulty in bleaching the TL-IRSL traps when the sediment includes more clay. The central part of the infilling is characterized by clastic clayey sediments coming from the Covacha de los Zarpazos area, which indicates that these sediments are composed of various deposits in the time and the space, thus implying a large variation of dose rate in a little space.

The TG8 level, appearing between the TG7 and TG9 layers, is not continuous throughout Galería. It consists of a thin clastic layer in which the surface area has been altered by a bat guano deposit. This organic layer has probably contributed to render the ESR-US ages younger than the true ages and provoking a complex post burial uranium uptake for teeth directly in contact with that layer. Small calcitic floors form at the base of TG8 and one of them yielded a U-series age older than 350 ka.

Bayesian modelling

In order to construct the chronological framework of the Galería site, several types of information are available, in particular stratigraphic context and radiometric dates. As usual, the stratigraphic context has been determined before performing different radiometric studies (ESR-US on teeth, TL and IRSL on sediments, U-series and ESR on calcite) on samples on which the stratigraphic location was well identified. Besides, radiometric measurements are defined by age distribution laws in an independent time-scale, to which is associated an uncertainty that can be more or less large. Because stratigraphic context on the one hand and radiometric data on the other hand derive from different and independent methods, we had to find a method to deal with the entire collection of data. As stratigraphic context was established before radiometric measurements, this information can be interpreted as a priori information to the radiometric measurements. By giving the terminology of a priori to this stratigraphic context, and likelihood to the radiometric measurements, we describe a Bayesian scheme; thus, both stratigraphy and radiometric dates can be combined to build a unique statistical model, using a Bayesian approach. This probabilistic approach allows the definition of a posteriori distribution laws combining stratigraphic context with radiometric information.

Consequently, in the following models, the stratigraphic information deduced from the archaeological excavations has been integrated as a priori to the radiometric probability densities, used as likelihood distributions, in order to determine a posteriori laws

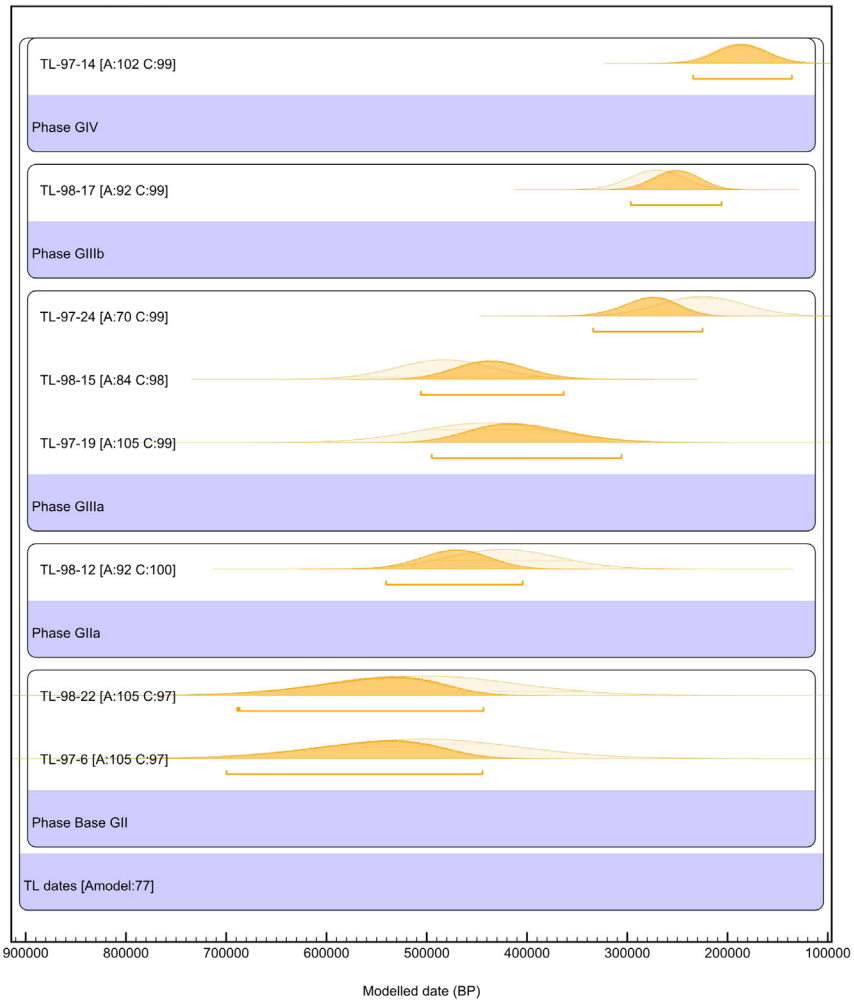

Figure 9. Bayesian modelling of luminescence dates (from Berger et al. (2008)). Probability densities are sequenced according to the stratigraphic context. A posteriori densities (deduced from the modelling) are shown in darker shade; the likelihoods (distribution laws deduced from the measurements, without any modelling) in lighter shade. This model is validated with an agreement of 77 (Amodel = 77): this chronostratigraphy is statistically possible.

Please cite this article in press as: Falguères, C., et al., Combined ESR/U-series chronology of Acheulian hominid-bearing layers at Trinchera Galería site, Atapuerca, Spain, Journal of Human Evolution (2013), http://dx.doi.org/10.1016/j.jhevol.2013.05.005

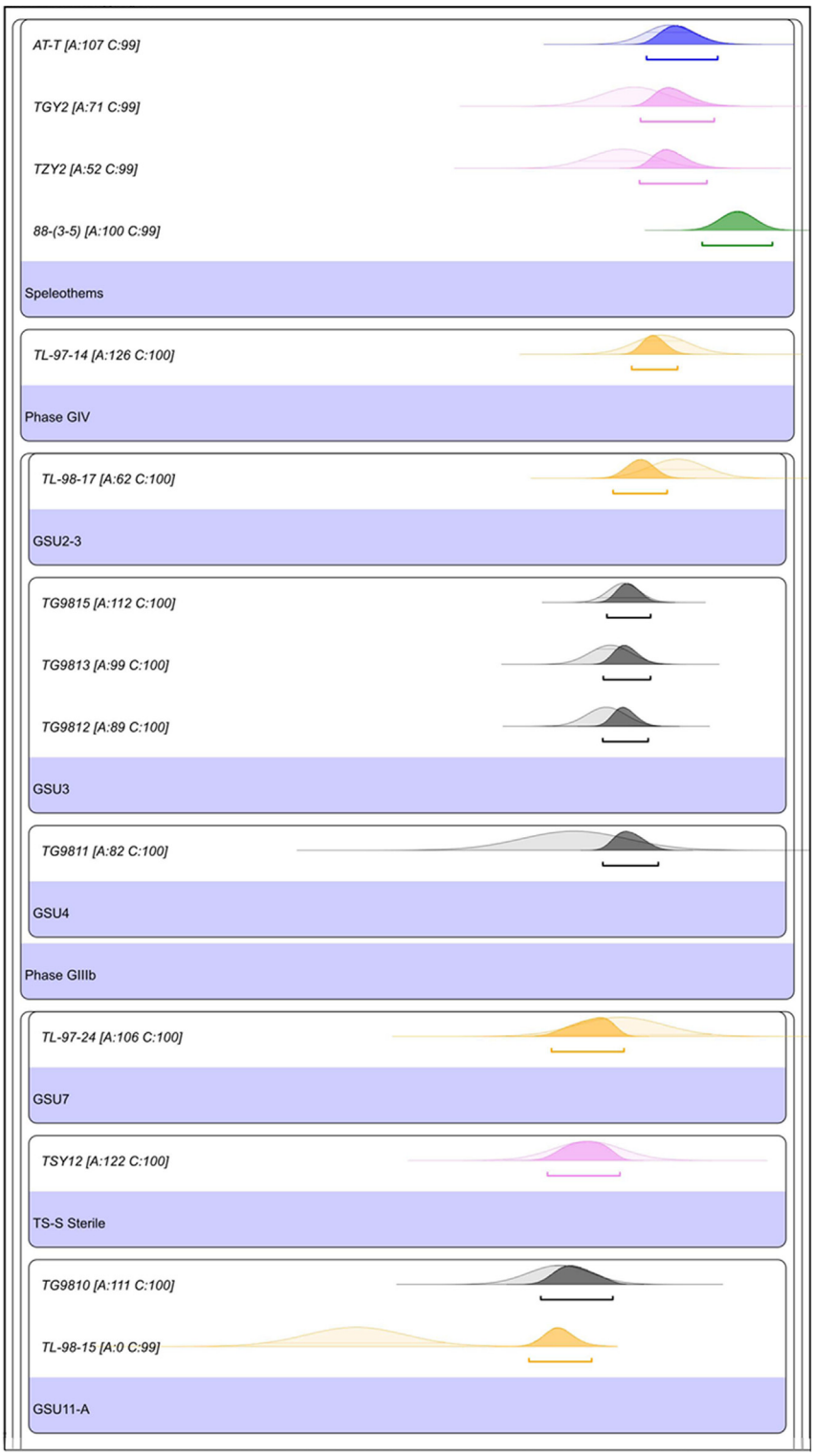

Figure 10. Chronological model for the Galería Stratigraphical Sequence. A posteriori densities (deduced from the modelling) are shown in darker shade; the likelihoods (distribution laws deduced from the measurements, without any modelling) in lighter shade. This model is not validated (Amodel = 7), TL-98-15 and TL-97-19 dates are identified as outliers. The model was re-run without these two OSL dates and it is validated (Amodel = 83): radiometric data are consistent stratigraphical units. U–Th on calcite dates are in green, ESR on calcite dates in violet, U–Th by ESR on calcite in blue, TL/IRSL in yellow and ESR-US on teeth in black. (For interpretation of the references to colour in this figure legend, the reader is referred to the web version of this article.)

Please cite this article in press as: Falguères, C., et al., Combined ESR/U-series chronology of Acheulian hominid-bearing layers at Trinchera Galería site, Atapuerca, Spain, Journal of Human Evolution (2013), http://dx.doi.org/10.1016/j.jhevol.2013.05.005

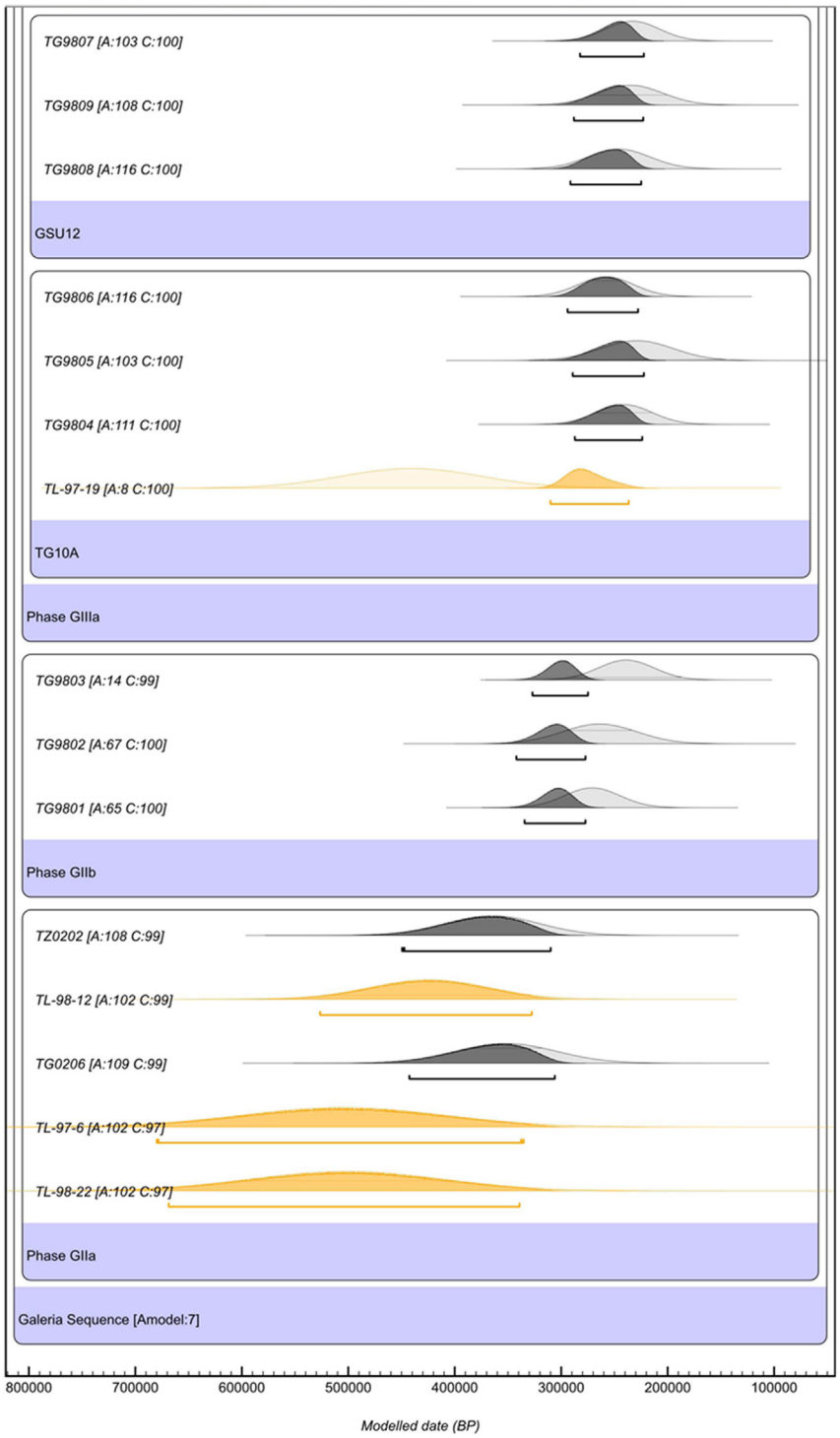

Figure 10. (*continued*).

incorporating all of the chonostratigraphical information that is available (Bronk Ramsey, 2001, 2009). Two units of priors have been used:

1) Prior Phase, which stands for an archaeological event without any chronological order between the dates it contains;
2) Prior Sequence, which sets a chronological order between the different events it contains (the events could be different dates or phases).

The following Bayesian models have been performed using OxCal 4.1.7 software. A posteriori laws have been validated using agreement and convergence factors following the terminology proposed in Bronk Ramsey (2009).

In this paragraph, the terminology of Phase and Sequence are used as explained above. According to the established stratigraphic context, a first Bayesian model using the latest ESR-US dates has been built. Dates have been incorporated in four different statistical phases called 'Phase GIIa', 'Phase GIIb', 'Phase GIIIa', 'Phase GIIb',

Please cite this article in press as: Falguères, C., et al., Combined ESR/U-series chronology of Acheulian hominid-bearing layers at Trinchera Galería site, Atapuerca, Spain, Journal of Human Evolution (2013), http://dx.doi.org/10.1016/j.jhevol.2013.05.005

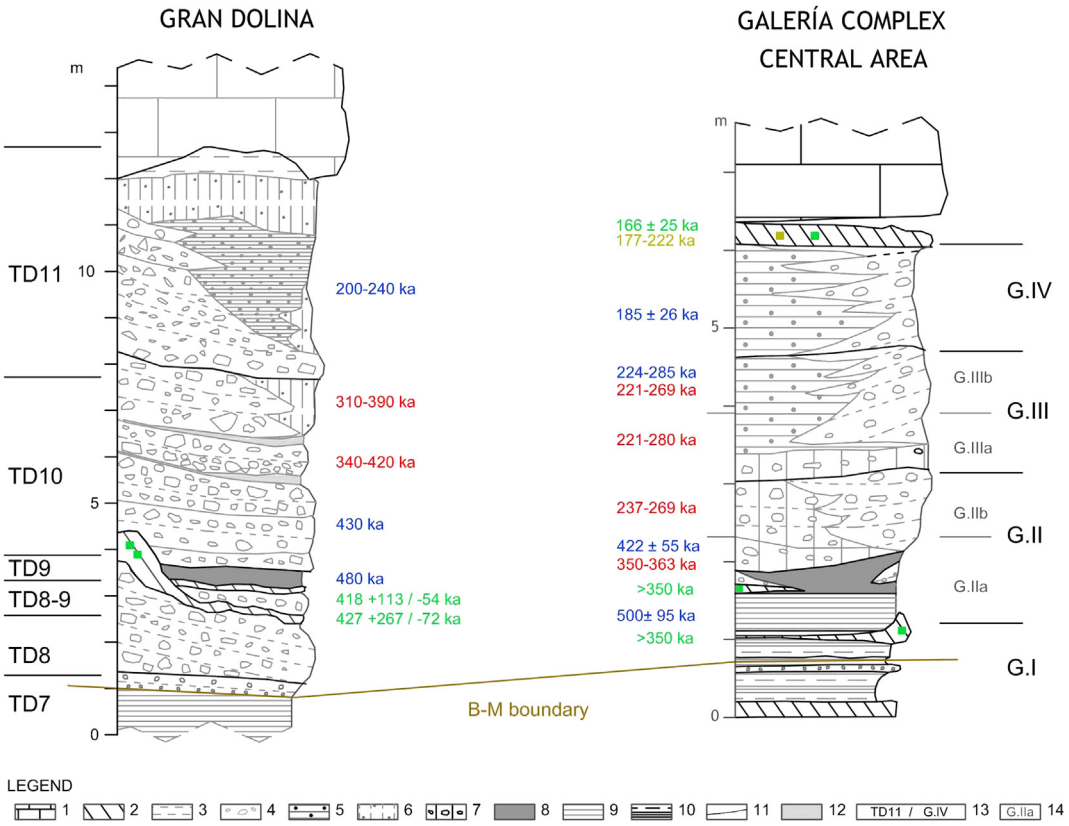

Figure 11. Chronostratigraphic correlation between upper part of Dolina and Galería sequence. U–Th ages are in green and brown; TL-IRSL ages are in blue; ESR-US ages are in red. Caption: 1) Upper Cretaceous limestone and dolomite (wall and roof of caves); 2) Speleothems; 3) Terra rossa; 4) Limestone blocks, cobbles and gravels; 5) Alternance of fine and medium pebbles and clay loam; 6) Lutites, clay loam; 7) Gravels and clay loam; 8) Bat guano and clay loam; 9) Laminated loamy clay; 10) Laminated sandy clay; 11) Main stratigraphical unconformities; 12) Main continuous archaeological levels; 13) Allostratigraphic units; 14) Archaeo-palaeontological levels. (For interpretation of the references to colour in this figure legend, the reader is referred to the web version of this article.)

and then GIII phases have been sub-divided following the stratigraphic units (Fig. 7). These phases were then sequenced, postulating the chronological succession: 'Phase GIIa' older than 'Phase GIIb' older than 'Phase GIIIa' older than 'Phase GIIIb' (Fig. 8). The 16 validated ESR-US dates are homogeneous from GIIa to GIIIb and range continuously from 450 to 170 ka without any statistical gap. The chronological sequence is accepted with an agreement of 94 (Amodel = 94), which confirms that the ESR-US dates and stratigraphic context concur.

Luminescence dates from the Galería stratigraphic sequence (Berger et al., 2008) are reported by integrating them in five phases ('Phase Base GII', 'Phase GIIa', 'Phase GIIIa', 'Phase GIIIb', 'Phase GIV'). Fig. 9 shows that the chronological frame is consistent. Nonetheless, we observe that dates move abruptly from around 400 to 250 ka between 'Phase GIIIa' and 'Phase GIIIb'. We then sequenced the previous model and we obtained an a posteriori model validated with an agreement of 77 (Amodel = 77, Fig. 9). Therefore, such a chronostratigraphy is statistically possible according to 1) the stratigraphic context, and 2) the TL physical measurements and in spite of the gap between 'Phase GIIIa' and 'Phase GIIIb'. This can be explained by the large uncertainty on these TL dates (between 10 and 19% for TL dates whereas uncertainty on ESR-US dates extends from 5 to 13% with one sigma error range).

Finally, we incremented the model by integrating ESR-US on teeth, U/Th and ESR on calcite and luminescence dates on sediments in the different phases, according to the stratigraphic units. AT-B in 'Phase GI' and 93-1 samples exhibit an isotopic equilibrium and suggest a great antiquity but are not representative in terms of age and should not be taken into account in the model. Fig. 10 shows that the radiometric data are not consistent since the Amodel = 7 and two TL dates are clearly rejected (TL97-19 and TL98-15, with an Ai = 8 and 0). The model has been re-run without these two oldest TL dates of 'Phase GIIIa'; the deduced model is validated (Amodel = 83) and shows that the Galería stratigraphical sequence and the radiometric dates (ESR-US, TL, U/Th) statistically concur.

Conclusions

The present ESR dates agree with the earlier luminescence dates and the other radiometric data for the upper part of the stratigraphic sequence (GIV and GIIIb). The ages obtained on teeth are homogeneous on GIII and GIIb units and range between 200 and 300 ka while TL ages change abruptly from 200 to 400 ka on the top of GIIIa.

In GIIa, two groups of ESR-US ages are observed. The first is in agreement with the TL ages ranging between 350 and 450 ka. The second group yields ages too young for TG8 and TN2B, which could be due to the presence of a bat guano layer in contact with these samples. This level could have played a role in the uranium mobility after burial though the *p*-values do not exhibit a post- burial uranium uptake responsible of the young ages. This outlines a complex geochemical history of these samples, which likely underwent first a uranium leaching followed by a recent uranium uptake.

If we consider that the first group yields reasonable ages, this would place the GIIa unit as contemporaneous with TD10 at Gran Dolina for which new ESR data on quartz yield a mean age of about

Please cite this article in press as: Falguères, C., et al., Combined ESR/U-series chronology of Acheulian hominid-bearing layers at Trinchera Galería site, Atapuerca, Spain, Journal of Human Evolution (2013), http://dx.doi.org/10.1016/j.jhevol.2013.05.005

420 ka (Moreno et al., in prep.). A stalagmitic floor located at the top of the TD8 level has provided two TIMS ages (performed at the GEOTOP of Montreal, Unpublished data) ranging between 400 and 450 ka, which could be coeval with the stalagmites formed at the basis of the TG8 level for which a U-series analysis has provided an isotopic equilibrium (age older than 350 ka) (Fig. 11).

Two human remains have been unearthed from Galería. One cranial fragment was found at the entrance of Covacha de los Zarpazos, likely at the bottom of GIIIa (Arsuaga et al., 1999). The second is the mandible fragment AT76-T1H found in 1976 and attributed to the GII unit (Rosas and Bermúdez de Castro, 1999). According to the authors, it presents similar morphology with human mandibles found at Sima de los Huesos. The radiometric ages proposed for GIIa place this fossil a little bit younger than the new chronology proposed for Sima de los Huesos, older than 500 ka (Bischoff et al., 2007), though this age is actually under revision but in agreement with ESR-US age of around 300 ka derived from bones (Bischoff et al., 1997).

Finally, new radiometric data presented here provide information that contribute to establish chronostratigraphical correlations among the different sites of Trinchera Atapuerca, documenting more than one million years of human occupation in this part of Europe.

Acknowledgements

We dedicate this paper to Glenn Berger with whom we spent good time sampling, talking about results and measuring external dose in different layers of Dolina at Atapuerca.

We thank Yuji Yokoyama for having provided unpublished data about gamma-ray spectrometric dating of human remains. We thank Rainer Grün for having improved the scientific content of this paper. We thank all the members of Atapuerca team, too numerous to be cited, who participated and contributed to finalize this paper. Research has been developed in the framework of the Spanish MICINN project CGL2009-12703-C03, the Catalan AGAUR projects 2009SGR-188 and 2009SGR-324 and Junta de Castilla y León.

References

Adamiec, G., Aitken, M.J., 1998. Dose-rate conversion factors: update. Ancient TL 16, 37–50.

Arsuaga, J.L., Gracia, A., Lorenzo, C., Martínez, I., Perez, P.J., 1999. Resto craneal humano de Galería/cueva de Zarpazos (Sierra de Atapuerca, Burgos). Arqueología en Castilla y León. Memorias 7, 233–235.

Bahain, J.J., Yokoyama, Y., Falguères, C., Sarcia, M.N., 1992. ESR dating of tooth enamel: a comparison with K-Ar dating. Quatern. Sci. Rev. 11, 245–250.

Bahain, J.J., Falguères, C., Laurent, M., Voinchet, P., Dolo, J.M., Antoine, P., Tuffreau, A., 2007. ESR chronology of the Somme River Terrace system and first human settlements in Northern France. Quatern. Geochronol. 2, 356–362.

Benito-Calvo, A., 2004. Análisis geomorfológico y reconstrucción de paleopaisajes neógenos y cuaternarios en la Sierra de Atapuerca y el valle medio del río Arlanzón. Universidad Complutense de Madrid. Ph.D Dissertation.

Benito-Calvo, A., Pérez-González, A., Parés, J.M., 2008. Quantitative reconstruction of Late Cenozoic landscapes: a case study in the Sierra de Atapuerca (Burgos, Spain). Earth Surf. Proc. Land. 33, 196–208.

Berger, G.W., Pérez-González, A., Carbonell, E., Arsuaga, J.L., Bermúdez de Castro, J.M., Ku, T.L., 2008. Luminescence chronology of cave sediments at the Atapuerca palaeoanthropological site, Spain. J. Hum. Evol. 55, 300–311.

Bermúdez de Castro, J.M., Arsuaga, J.L., Carbonell, E., Rosas, A., Martínez, I., Mosquera, M., 1997. A hominid from the Lower Pleistocene of Atapuerca, Spain: possible ancestor to Neadertals and modern humans. Science 276, 1392–1395.

Bermúdez de Castro, J.M., Martinón-Torres, M., Lozano, M., Sarmiento, S., Muela, A., 2004. Paleodemography of the Atapuerca-Sima de los Huesos hominin sample: a revision and new approaches to the paleodemography of the European Middle Pleistocene population. J. Anthropol. Res. 60, 5–26.

Bermúdez de Castro, J.M., Martinón-Torres, M., Gómez-Robles, A., Prado-Simón, L., Martín-Francés, L., Lapresa, M., Olejniczak, A., Carbonell, E., 2011. Early Pleistocene human mandible from Sima del Elefante (TE) cave site in Sierra de Atapuerca (Spain): a comparative morphological study. J. Hum. Evol. 61, 12–25.

Bischoff, J.L., Rosenbauer, R.J., Tavoso, A., de Lumley, H., 1988. A test of uranium-series dating of fossil tooth enamel: results from Tournal cave, France. Appl. Geochem. 3, 135–141.

Bischoff, J.L., Fitzpatrick, J.A., León, L., Arsuaga, J.L., Falguères, C., Bahain, J.J., Bullen, T., 1997. Geology and preliminary dating of the hominid-bearing sedimentary fill of the Sima de los Huesos chamber, Cueva Mayor of the Sierra de Atapuerca, Burgos, Spain. J. Hum. Evol. 33, 129–154.

Bischoff, J.L., Williams, R.W., Rosenbauer, R.J., Aramburu, A., Arsuaga, J.L., García, N., Cuenca-Bescós, G., 2007. High-resolution U-series dates from the Sima de los Huesos hominids yields 600 $+\infty$/-66 kyrs: implications for the evolution of the early Neanderthal lineage. J. Archaeol. Sci. 34, 763–770.

Bronk Ramsey, C., 2001. Development of the radiocarbon calibration program. Radiocarbon 43, 355–363.

Bronk Ramsey, C., 2009. Bayesian analysis of Radiocarbon dates. Radiocarbon 51, 337–360.

Carbonell, E., Esteban, M., Martín Najera, A., Mosquera, M., Rodriguez, X.P., Olle, A., Sala, R., Verges, J.M., Bermúdez de Castro, J.M., Ortega, A.I., 1999a. The Pleistocene site of Gran Dolina, Sierra de Atapuerca, Spain: a history of the archaeological investigations. J. Hum. Evol. 37, 313–324.

Carbonell, E., Rosas, A., Díez, J.C. (Eds.), 1999b. Atapuerca: Ocupaciones Humanas y Palaeoecología del Yacimiento de Galería. Arqueología en Castilla y León, Memorias 7. Junta de Castilla y León, Valladolid.

Carbonell, E., Mosquera, M., Ollé, A., Rodríguez, X.P., Sala, R., Vergès, J.M., Arsuaga, J.L., Bermúdez de Castro, J.M., 2003. Les premiers comportements funéraires auraient-ils pris place à Atapuerca, il y a 350 000 ans? L'Anthropologie 107, 1–14.

Carbonell, E., Bermúdez de Castro, J.M., Parés, J.M., Pérez-González, A., Cuenca-Bescós, G., Ollé, A., Mosquera, M., Huguet, R., Made, J., van der, Rosas, A., Sala, R., Vallverdú, J., García, N., Granger, D.E., Martinón-Torres, M., Rodríguez, X.P., Stock, G.M., Vergès, J.M., Allué, E., Burjachs, F., Cáceres, I., Canals, A., Benito, A., Díez, C., Lozano, M., Mateos, M., Navazo, M., Rodríguez, J., Rosell, J., Arsuaga, J.L., 2008. The first hominin of Europe. Nature 452, 465–470.

Chabaux, F., Dequincey, O., Lévèque, J.J., Leprun, J.C., Clauer, N., Riotte, J., Paquet, H., 2003. Tracing and dating recent chemical transfers in weathering profiles by trace element geochemistry and 238U–234U–230Th disequilibria: the example of the Kaya lateritic toposequence (Burkina-Faso). C. R. Geosci. 335, 1219–1231.

Cuenca-Bescós, G., Laplana, C., Canudo, J.I., 1999. Biochronological implications of the Arvicolidae and Cricetidae (Rodentia, Mammalia) from the Lower Pleistocene hominid bearing level Trinchera Dolina 6 (TD6, Atapuerca, Spain). J. Hum. Evol. 37, 353–373.

Cuenca-Bescós, G., Rofes, J., Lopez-García, J.M., Blain, H.A., De Marfa, R.J., Galindo-Pellicena, M.A., Bennasar-Serra, M.L., Melero-Rubio, M., Arsuaga, J.L., Bermúdez de Castro, J.M., Carbonell, E., 2010. Biochronology of Spanish Quaternary small vertebrate faunas. Quatern. Int. 212, 109–119.

Falguères, C., 1986. Datations de sites acheuléens et moustériens du midi méditerranéen par la méthode de résonance de spin Electronique. Muséum national d'histoire naturelle, Paris. Ph.D. Dissertation.

Falguères, C., Bahain, J.J., Yokoyama, Y., Arsuaga, J.L., Bermúdez de Castro, J.M., Carbonell, E., Bischoff, J.L., Dolo, J.M., 1999. Earliest humans in Europe: the age of TD6 Gran Dolina, Atapuerca, Spain. J. Hum. Evol. 37, 343–352.

Falguères, C., Bahain, J.J., Duval, M., Shao, Q., Han, F., Lebon, M., Mercier, N., Pérez-González, A., Dolo, J.M., Garcia, T., 2010. A 300-600 ka ESR/U-series chronology of Acheulian sites in Western Europe. Quatern. Int. 223–224, 293–298.

García, N., 2003. Osos y Otros Carnívoros de la Sierra de Atapuerca. Fundación Osos de Asturias, Oviedo.

García, N., Arsuaga, J.L., Torres, T., 1997. The carnivore remains from the Sima de los Huesos Middle Pleistocene site (Sierra de Atapuerca, Spain). J. Hum. Evol. 33, 155–174.

Grün, R., 2009a. The relevance of parametric U-uptake models in ESR age calculations. Radiat. Meas. 44, 472–476.

Grün, R., 2009b. The DATA program for the calculation of ESR age estimates on tooth enamel. Quatern. Geochronol. 4, 231–232.

Grün, R., Aguirre, E., 1987. Datacion por ESR y por la serie de1 U, en los depositos cársticos de Atapuerca. In: Aguirre, E., Carbonell, E., Bermúdez de Castro, J.M. (Eds.), El Hombre Fósil de Ibeas y el Pleistoceno de la Sierra de Atapuerca. Junta de Castilla y León, Valladolid, pp. 201–204.

Grün, R., Katzenberger-Apel, O., 1994. An alpha irradiator for ESR dating. Ancient TL 12, 35–38.

Grün, R., Schwarcz, H.P., Chadam, J.M., 1988. ESR dating of tooth enamel: coupled correction for U-uptake and U-series disequilibrium. Nucl. Tracks Rad. Meas. 14, 237–241.

Grün, R., Joannes-Boyau, R., Stringer, C., 2008. Two types of CO^{2-} radicals threaten the fundamentals of ESR dating of tooth enamel. Quatern. Geochronol. 3, 150–172.

Marsh, R., 1999. Beta-gradient Isochrons Using Electron Paramagnetic Resonance: Towards a New Dating Method in Archaeology. McMaster University. Ph.D. Dissertation.

Moreno, D., Falguères, C., Pérez-González, A., Duval, M., Voinchet, P., Benito-Calvo, A., Ortega, A.I., Bahain, J.J., Sala, R., Carbonell, E., Bermúdez de Castro, J.M., Arsuaga, J.L., 2012. ESR chronology of alluvial deposits in the Arlanzón valley (Atapuerca, Spain): contemporaneity with Atapuerca Gran Dolina site. Quatern. Geochronol. 10, 418–423.

Ollé, A., Mosquera, M., Rodríguez, X.P., de Lombera-Hermida, A., García-Antón, M.D., García-Medrano, P., Peña, L., Menéndez, L., Navazo, M., Terradillos, M., Bargalló, A., Márquez, B., Sala, R., Carbonell, E., 2013. The Early and Middle Pleistocene technological record from Sierra de Atapuerca (Burgos, Spain). Quatern. Int. 295, 138–167.

Please cite this article in press as: Falguères, C., et al., Combined ESR/U-series chronology of Acheulian hominid-bearing layers at Trinchera Galería site, Atapuerca, Spain, Journal of Human Evolution (2013), http://dx.doi.org/10.1016/j.jhevol.2013.05.005

Ortega, A.I., 2009. La evolución geomorfológica del karst de la Sierra de Atapuerca (Burgos) y su relación con los yacimientos pleistocenos que contiene. University of Burgos. Ph.D. Dissertation.

Ortega, A.I., Benito-Calvo, A., Pérez-González, A., Martín Merino, M.A., Pérez Martínez, R., Parés, J.M., Aramburu, A., Arsuaga, J.L., Bermúdez de Castro, J.M., Carbonell, E., 2012. Evolution of multilevel caves in the Sierra de Atapuerca (Burgos, Spain) and its relation to human occupation. Geomorphology. http://dx.doi.org/10.1016/j.geomoph.2012.05.031. in press.

Osmond, J.K., Ivanovich, M., 1992. Uranium-series mobilization and surface hydrology. In: Ivanovich, M., Harmon, R.S. (Eds.), Uranium-series Disequilibrium: Applications to Earth, Marine and Environmental Sciences, second ed. Clarendon Press, Oxford, pp. 259–288.

Parés, J.M., Pérez-González, A., 1995. Palaeomagnetic age for hominid fossils at Atapuerca archaeological site. Spain. Sci. 269, 830–832.

Parés, J.M., Pérez-González, A., 1999. Magnetochronology and stratigraphy at Gran Dolina section, Atapuerca (Burgos, Spain). J. Hum. Evol. 37, 325–342.

Parés, J.M., Pérez-González, A., Rosas, A., Benito, A., Bermúdez de Castro, J.M., Carbonell, E., Huguet, R., 2006. Matuyama-age lithic tools from the Sima del Elefante site, Atapuerca (northern Spain). J. Hum. Evol. 50, 163–169.

Pérez-González, A., Aleixandre, T., Pinilla, A., Gallardo, J., Benayas, J., Martínez, M.J., Ortega, A.I., 1995. Aproximación a la estratigrafía de Galería en la Trinchera de Atapuerca (Burgos). In: Aguirre, E., Carbonell, E., Bermúdez de Castro, J.M. (Eds.), Evolución Humana en Europa y los Yacimientos de la Sierra de Atapuerca. Junta de Castilla y León, Valladolid, pp. 99–122.

Pérez-González, A., Parés, J.M., Gallardo, J., Aleixandre, T., Ortega, A.I., Pinilla, A., 1999. Geología y estratigrafía del relleno de Galería de la Sierra de Atapuerca (Burgos). Arqueologia en Castilla y León, Memorias 7, 31–42.

Pérez-González, A., Parés, J.M., Carbonell, E., Aleixandre, T., Ortega, A.I., Benito, A., Martín Merino, M.A., 2001. Géologie de la Sierra de Atapuerca et stratigraphie des remplissages karstiques de Galería et Dolina (Burgos, Espagne). L'Anthropologie 105, 27–43.

Pineda, A., Arce, J.M., 1997. Mapa Geológico del España escala 1:50.000, 2a Serie (MAGNA). Hoja de Burgos, 200 (19-10). IGME. Serv. Pub. M° Industria, Madrid.

Rodríguez, J., Burjachs, F., Cuenca-Bescós, G., García, N., Made, J.v.d., Pérez-González, A., Blain, H., Expósito, I., López-García, J.M., García Antón, M., Allué, E., Cáceres, I., Huguet, R., Mosquera, M., Ollé, A., Rosell, J., Parés, J.M., Rodríguez, X.P., Díez, J.C., Rofes, J., Sala, R., Saladié, P., Vallverdú, J., Bennàsar, M.L., Blasco, R., Bermúdez de Castro, J.M., Carbonell, E., 2011. One million years of cultural evolution in a stable environment at Atapuerca (Burgos, Spain). Quatern. Sci. Rev. 30, 1396–1412.

Rosas, A., Bermúdez de Castro, J.M., 1999. Descripción y posición evolutiva de la mandíbula AT76-T1H del yacimiento de Galería (Sierra de Atapuerca). Arqueología en Castilla y León, Memorias 7, 237–243.

Stringer, C., 2012. The status of *Homo heidelbergensis* (Schoentensack, 1908). Evol. Anthropol. 21, 101–107.

Vallverdu, J., 1999. Micromorfología de las facies sedimentarias de la Sierra de Atapuerca y del nivel J del Abric Romanií. Implicaciones geoarqueológicas y paleoetnográficas. University Rovira i Virgili. Ph.D. Dissertation.

Yokoyama, Y., Falguères, C., Quaegebeur, J.P., 1985. ESR dating of quartz from Quaternary sediments: first attempt. Nucl. Tracks Rad. Meas. 10, 921–928.

Yokoyama, Y., Nguyen, H.V., 1980. Direct and non destructive dating of marine sediments, manganese nodules and corals by high resolution gamma-ray spectrometry. In: Saruhashi, K., Goldberg, E.D., Horibe, Y. (Eds.), Isotope Marine Chemistry. Uchida Rokakuho, Tokyo, pp. 259–289.

Please cite this article in press as: Falguères, C., et al., Combined ESR/U-series chronology of Acheulian hominid-bearing layers at Trinchera Galería site, Atapuerca, Spain, Journal of Human Evolution (2013), http://dx.doi.org/10.1016/j.jhevol.2013.05.005